Journal of Visualized Experiments

Measuring nucleotide binding to intact, functional membrane proteins in real time

--Manuscript Draft--

Article Type:	Invited Methods Article - JoVE Produced Video
Manuscript Number:	JoVE61401R1
Full Title:	Measuring nucleotide binding to intact, functional membrane proteins in real time
Section/Category:	JoVE Biochemistry
Keywords:	Ligand binding; membrane protein; ion channel; nucleotide; method; Patch clamp; fluorescence; spectra; receptor
Corresponding Author:	Michael Christian Puljung, Ph.D. University of Oxford Oxford, Oxfordshire UNITED KINGDOM
Corresponding Author's Institution:	University of Oxford
Corresponding Author E-Mail:	michael.puljung@dpag.ox.ac.uk
Order of Authors:	Samuel G. Usher
	Frances M. Ashcroft
	Michael Christian Puljung, Ph.D.
Additional Information:	
Question	**Response**
Please indicate whether this article will be Standard Access or Open Access.	Open Access (US$4,200)
Please indicate the **city, state/province, and country** where this article will be **filmed**. Please do not use abbreviations.	Oxford, Oxfordshire, United Kingdom

TITLE:

Measuring Nucleotide Binding to Intact, Functional Membrane Proteins in Real Time

AUTHORS AND AFFILIATIONS:

Samuel G. Usher[1], Frances M. Ashcroft[1], Michael C. Puljung[1,2]

[1]Department of Physiology, Anatomy and Genetics, University of Oxford, Oxford UK
[2]Current address: Department of Chemistry and Neuroscience Program, Trinity College, Hartford, CT, USA,

Corresponding authors:
Frances M. Ashcroft (frances.ashcroft@dpag.ox.ac.uk)
Michael C. Puljung (michael.puljung@dpag.ox.ac.uk; michael.puljung@trincoll.edu)

Email Addresses of Co-Authors:
Samuel G. Usher (samuel.usher@gtc.ox.ac.uk)

KEYWORDS:

ligand binding, membrane protein, ion channel, nucleotide, method, patch clamp, fluorescence, spectra, receptor

SUMMARY:

This protocol presents a method for measuring adenine nucleotide binding to receptors in real time in a cellular environment. Binding is measured as Förster resonance energy transfer (FRET) between trinitrophenyl nucleotide derivatives and protein labeled with a non-canonical, fluorescent amino acid.

ABSTRACT:

We have developed a method to measure binding of adenine nucleotides to intact, functional transmembrane receptors in a cellular or membrane environment. This method combines expression of proteins tagged with the fluorescent non-canonical amino acid ANAP, and FRET between ANAP and fluorescent (trinitrophenyl) nucleotide derivatives. We present examples of nucleotide binding to ANAP-tagged K_{ATP} ion channels measured in unroofed plasma membranes and excised, inside-out membrane patches under voltage clamp. The latter allows for simultaneous measurements of ligand binding and channel current, a direct readout of protein function. Data treatment and analysis are discussed extensively, along with potential pitfalls and artefacts. This method provides rich mechanistic insights into the ligand-dependent gating of K_{ATP} channels and can readily be adapted to the study of other nucleotide-regulated proteins or any receptor for which a suitable fluorescent ligand can be identified.

INTRODUCTION:

Several important classes of protein are directly regulated by ligand binding. These range from soluble enzymes to membrane-embedded proteins including receptor tyrosine kinases, G protein-coupled receptors (GPCRs), and ion channels. GPCRs and channels account for ~34% and ~15% of all current drug targets, respectively[1,2]. Therefore, there is a considerable biochemical, as well as medical interest in developing methods that provide mechanistic

insights into ligand-receptor interactions. Traditional methods for measuring ligand binding, including photoaffinity labeling and radioligand binding studies, require large amounts of partially purified protein and are typically performed under non-physiological conditions and time scales. An ideal method would require only small amounts of protein, could be performed on intact proteins expressed in a cellular or membrane environment, could be monitored in real time, and would be compatible with direct readouts of protein function.

Förster resonance energy transfer (FRET) is a method that detects the proximity between two fluorescently tagged molecules[3]. FRET occurs when an excited donor fluorophore transfers energy in a non-radiative fashion to an acceptor molecule (typically another fluorophore). Energy transfer results in quenching of the donor fluorescence emission and sensitization of the acceptor emission (if the acceptor is a fluorophore). Transfer efficiency is dependent on the 6^{th} power of the distance between the donor and the acceptor. Furthermore, the donor and acceptor must be in proximity (usually less than 10 nm) for FRET to occur. As such, FRET can be exploited to measure the direct binding between a fluorescently labeled protein receptor and a fluorescent ligand.

Several different proteins are regulated or activated by binding intracellular or extracellular adenine nucleotides (ATP, ADP, AMP, cAMP). Many transporter proteins require ATP hydrolysis for their reaction cycle, including ATP-binding cassette transporters and P-type ATPases like the Na^+/K^+ pump[4,5]. ATP-sensitive K^+ (K_{ATP}) channels, the cystic fibrosis transmembrane conductance regulator (CFTR), and cyclic-nucleotide regulated channels are all ion channels that are gated by the binding of intracellular adenine nucleotides, making them exquisitely sensitive to changes in cellular metabolism and signal transduction[6-8]. Purinergic P2X and P2Y receptors respond to changes in extracellular ATP, which can be released as a neurotransmitter or as a result of tissue damage[9]. We have developed a FRET-based assay for the measurement of adenine nucleotide binding to membrane proteins in real time. We have previously applied this method to study nucleotide binding to K_{ATP} channels[10,11].

To measure nucleotide binding via FRET, a protein of interest must first be tagged with a fluorophore. The fluorescent tag must be inserted site-specifically in the protein of interest such that it is close enough to the ligand binding site for FRET to occur, with special care taken to ensure that the tag does not affect the protein's overall structure and function. To accomplish this, we employ a technique developed by Chatterjee et al., using amber stop-codon suppression to insert a fluorescent non-canonical amino acid (L-3-(6-acetylnaphthalen-2-ylamino)-2-aminopropionic; ANAP) at the desired site[12]. We measure nucleotide binding as FRET between ANAP-labeled protein and fluorescent, trinitrophenyl (TNP) nucleotide derivatives (**Figure 1A**). The emission spectrum for ANAP overlaps with the absorbance spectrum of TNP-nucleotides, a condition necessary for FRET to occur (**Figure 1B**). Here we outline two different types of binding experiment. In the first, nucleotide binding to the intracellular side of ANAP-labeled K_{ATP} channels is measured in cells that have been unroofed by sonication leaving adherent fragments of plasma membrane on a glass cover slip[10,11,13,14].

In the second method, nucleotide binding to ANAP-labeled K_{ATP} channels is measured in a membrane patch under voltage clamp, allowing for the simultaneous measurement of ionic currents and fluorescence. By combining these two experimental approaches, changes in

binding can be directly correlated with changes in channel function[11]. Typical results, potential pitfalls, and data analysis are discussed.

PROTOCOL:

1. Preparation of cover slips

NOTE: These steps must take place in a tissue-culture hood. Quantities are given for the preparation of 10 dishes.

1.1. Place ten autoclaved, 30 mm borosilicate cover glass slips individually into ten 35 mm non-treated sterile dishes and rinse once with 2 mL of sterile, distilled water.

1.2. Dilute 1 mL of 0.1% w/v poly-L-lysine solution into sterile, distilled water to a total volume of 10 mL (final concentration of 0.01% w/v). Mix well, then pipette 1 mL onto each cover slip and incubate at room temperature for 20 min.

1.3 Aspirate the poly-L-lysine and wash each cover slip twice with at least 2 mL of sterile distilled water. Leave until completely dry i.e., at least 3 h.

2. Seeding HEK-293T cells

NOTE: These steps must take place in a tissue-culture hood. HEK-293T cells were chosen for their low current background and ease of growing in culture. This protocol may be adapted to other cell types.

2.1. Rinse an 80-90% confluent T75 flask of HEK-293T cells once with 12 mL phosphate buffered saline (PBS) before incubating with 2 mL trypsin for 2-5 min, or until the cells are fully detached and almost completely dissociated.

2.2. Resuspend the cells by adding 10 mL Dulbecco's Modified Eagle Medium (DMEM) supplemented with 10% fetal bovine serum, 100 U/mL penicillin and 100 µg/mL streptomycin. Pipette gently against the bottom of the flask to break up remaining clumps of cells.

2.3. Add 2 mL of supplemented DMEM to the desired number of 35 mm dishes containing coated cover slips. Add 100 µL of resuspended cells to each dish. Incubate overnight at 37 ˚C.

3. Transfection

NOTE: These steps must take place in a tissue-culture hood. Quantities are given for the transfection of 10 dishes. For site-specific ANAP incorporation, the DNA codon at the position intended for labeling must be replaced with the amber (TAG) stop codon. This construct is co-transfected with two plasmids: pANAP and peRF1-E55D[12,15]. pANAP encodes several copies of an ANAP-specific tRNA/tRNA synthetase pair. In the presence of ANAP, transfection of this plasmid produces tRNA charged with ANAP that recognizes the amber stop codon. peRF1-E55D encodes a dominant negative ribosomal release factor that increases the yield of full-length, ANAP-tagged protein.

3.1. Prepare a 1.5 mL tube with 10 µg pANAP, 10 µg peRF1-E55D, and DNA for the construct intended for labeling with ANAP. Bring to a final volume of 500 µL with unsupplemented DMEM.

3.2. In a separate tube, prepare 3 µL of lipid-based transfection reagent (see **Table of Materials**) for each 1 µg of DNA and bring to a final volume of 500 µL with unsupplemented DMEM.

3.3. Combine the DNA and transfection reagent mixtures in a single tube and incubate for 20 min at room temperature.

3.4. Add 400 µL of the 1 mM ANAP stock (trifluoroacetate salt in 30 mM NaOH) to 20 mL supplemented DMEM for a final concentration of 20 µM ANAP. Replace the old media from the plated cells with 2 mL of the ANAP-containing media per dish.

3.5. Pipette 10% of the DNA transfection mix onto each dish. Incubate at 33 °C for 2-4 days before experiments. Incubation at 33 °C slows the cell division and increases the protein yield per cell[16].

4. Unroofed membrane experiments

4.1. Use a pair of forceps to break a cover slip with transfected cells into smaller fragments.

4.2.1. Follow one of the procedures below to unroof cells.

4.2.1. If using pre-coated cover slips, rinse a fragment with PBS, then place it on the bottom of a 35 mm dish containing 2 mL PBS. Briefly sonicate using a probe sonicator (50 W, 20%-40% amplitude, 3 mm probe) positioned 3-5 mm above the sample to unroof cells and leave behind adherent plasma membrane fragments (**Figure 2A,C**).

NOTE: Sonicator power, duration, and probe height above the sample can all be varied to obtain a high yield of unroofed membranes without completely denuding the coverslip.

4.2.2. If not using pre-coated cover slips, rinse a cover slip fragment with PBS, then dip into a tube containing 0.1% w/v poly-L-lysine for ~30 s before briefly sonicating (as in step 4.2.1) to unroof cells and leave behind unroofed/partially unroofed plasma membrane fragments (**Figure 2A,C,D**). Brief exposures to poly-L-lysine have been demonstrated to improve adherence to the coverslip[13].

4.3. Place the sonicated fragment into a cover glass-bottom 35 mm dish containing 2 mL bath solution and mount onto an inverted microscope equipped with a high NA, 60x water immersion objective. The camera port of the microscope is connected to a spectrograph in series with a high sensitivity CCD camera. Perfuse the bath chamber (0.5 – 1 mL/min) with buffer using a peristaltic pump. The composition of the buffer will vary depending on the protein under study.

NOTE: If the user does not have access to an objective with a long working distance, it may be impossible to focus on the unroofed membrane fragments due to the extra height of the cover slip. An alternative is to seed cells directly onto dishes with poly-L-lysine glass bottoms (see **Table of Materials** for an example). This will also reduce potential aberrations in the image associated with focusing through two pieces of glass. These aberrations do not affect the shape of the spectra acquired.

4.4. Identify unroofed membrane fragments expressing the ANAP-labeled channel by looking for channel fluorescence (**Figure 2C,D**).

NOTE: It is recommended to use an additional fluorescent label (where the emission spectrum is distinguishable from the ANAP emission spectrum) to help identify unroofed membranes containing the protein of interest. The experiments in **Figure 2C,D** were performed on ANAP-labeled channels with C-terminal fluorescent protein tags.

4.5 Partially engage the spectrometer mask (raise ~10%) between the camera port on the microscope and the spectrograph. The shadow of the mask will appear on the camera image. Align the unroofed membrane with the spectrometer mask, by adjusting the microscope stage. Acquire a bright field and fluorescence image of the unroofed membrane. These will be used to select a region of interest for analysis.

4.6. Bring the tip of the microvolume perfusion system close to the unroofed membrane.

NOTE: To reduce the background fluorescence, the outflow of the perfusion system was replaced with a custom tip made from borosilicate glass.

4.7. To image fluorescence spectra, excite the membrane with a 385 nm LED through a 390/18 nm band-pass excitation filter and a 416 nm edge dichroic. Collect emitted light through a 400 nm long-pass emission filter (**Figure 2B**).

4.8. Engage the spectrometer mask and ensure the emitted light is passed through. Engage the spectrometer gratings (300 grooves/mm). With the gratings in place, the light diffracted by the spectrometer will be projected onto the chip of the CCD camera to produce spectral images (**Figure 3A**). These images retain spatial information in the *y* dimension. The *x* dimension is replaced with wavelength.

4.9. Optionally, if the protein of interest is tagged with a fluorescent protein, acquire a spectral image of the fluorescent protein using the appropriate filter set.

4.10. Take one or more 0.1-10 s exposures at the start of the experiment while perfusing nucleotide-free buffer solution. These will be used to correct and normalize data throughout the rest of the experiment (see section 5 below).

NOTE: Choice of exposure time will depend on the expression level achieved, the brightness of the fluorophore, and the optics. Exposure time should be chosen to maximize signal and minimize the observed bleaching rate. The exposure time range given in 4.10 is suitable for equilibrium binding measurements but may be useful for measuring slower kinetic changes[10].

The ability to use short exposure times to track faster kinetics will be limited by protein expression levels and photobleaching, rather than hardware.

4.11. Apply a range of concentrations of TNP-ATP (usually prepared in bath solution) to establish a concentration-response curve. Perfuse each solution for at least 1 min to ensure that a steady state is reached and wash out each concentration with bath solution for at least 1 min.

NOTE: It is important to ensure that the perfusion system can rapidly reach equilibrium (**Figure 2E**) and achieve the correct local concentration of TNP-ATP (**Figure 2F**).

4.12. Take an exposure (with the same duration as used in step 4.10) at each concentration and at the end of each washout.

5. Spectral analysis

NOTE: These instructions are written for use with the analysis code "pcf.m", which can be found at GitHub. https://github.com/mpuljung/spectra-analysis[10]. Additional and alternative code can be found at https://github.com/smusher/KATP_paper_2019[11]. We have described the operations performed by the software here so that the user may create their own code or choose to analyze the data manually.

5.1. Start the analysis program by typing the program's name ("pcf") in the command line.

5.2. When, an open file/folder dialog box will open with the prompt: "**Select files for ROI**", select the file names associated with the brightfield and fluorescence images of the unroofed membrane. A prompt will appear in the command line to type the name of the output file.

5.3. Type the file name and hit enter.

5.4. When the software displays the brightfield and fluorescence images, select a region of interest (ROI) in the spectral image corresponding to the location of the unroofed membrane fragment or excised patch (see section 6) following the software prompts. Select a background region in the same spectral image (representing the same wavelength range as in the ROI) corresponding to a section of cover slip or dish with no membrane attached (**Figure 3A**). The software will prompt to click the Top of the **ROI** and press **Enter**, click the bottom of the **ROI** and press **Enter** and then repeat this process for the background region.

5.5. When an open file/folder dialog box will open with the prompt: "**Select File for FP Spectrum"**, select the file name associated with the fluorescent protein (FP) spectrum (optional step 4.9). If no FP spectrum was acquired, select a different spectrum file. The FP spectrum serves as quality control to distinguish between tagged protein and background fluorescence.

5.6. When an open file/folder dialog box will open with the prompt: "**Select Files for Analysis**", select all the files corresponding to the ANAP spectra (from steps 4.10 to 4.12), including the files needed for bleach correction.

5.7. When an open file/folder dialog box will open with the prompt: "**Select Files for Bleaching Collection**", select the subset of files from step 5.6 corresponding to initial spectra acquired in nucleotide-free solution at the beginning of the experiment or spectra acquired during washes in nucleotide-free solution to be used for correction (from steps 4.10 to 4.12).

5.8. Line-average each image to produce spectra, i.e., average the intensity for all pixels in the *y* dimension of an ROI or background region at each wavelength. (**Figure 3B**). Subtract the resulting averaged background spectrum from the averaged spectrum acquired from the ROI to remove background fluorescence and fluorescence from unbound TNP-ATP (**Figure 3C**). These steps are performed automatically by the software.

5.9. Determine the ANAP intensity for each exposure by averaging the intensity of a 5 nm window centered around the ANAP peak of the subtracted spectra (typically ~470 nm but may vary depending on the local microenvironment of the ANAP residue).

NOTE: **Figure 3D** shows 6 spectra obtained from consecutive 10 s exposures of an unroofed membrane fragment expressing ANAP-tagged channels. The inset shows the averaged intensity of the peak of each spectrum. The software will automatically find the peak wavelength in the first spectrum acquired and use this value throughout. The intensity will be calculated automatically by the software.

5.10. Normalize the ANAP intensities for each experiment by dividing the ANAP intensity of a given exposure (*F*) by the ANAP intensity of the first exposure in the time series, which was taken in step 4.8 (F_{max}). Again, the software performs these calculations automatically.

5.11. Perform the steps below to obtain data.

5.11.1. To correct for ANAP photobleaching, first fit a single exponential decay, $(F/F_{max}) = A*\exp(-t/\tau)+(1-A)$, where *t* is the cumulative exposure time, τ is the time constant and A is the amplitude) to either the intermediate wash steps between TNP-ATP applications or to multiple initial exposures taken before washing on TNP-ATP (Figure 3D, inset).

NOTE: The software will display this fit and prompt to accept or reject it. If the fit is rejected, another opportunity will be provided to select files for bleaching correction.

5.11.2. Divide the normalized (in step 5.4) ANAP spectra by the predicted value of the exponential fit from step 5.5 at each time point (**Figure 3E**).

NOTE: For the example shown, the observed normalized peak fluorescence at 50 s is 0.65 and the predicted fluorescence from the exponential fit is 0.64. To correct for bleaching, divide the observed value (0.65, **Figure 3E** inset, empty circle) by the predicted value (0.64, **Figure 3E inset**, dashed line) to produce the corrected value (~1, **Figure 3E** inset, colored circle). If bleaching correction is adequate, the intensity of ANAP from all exposures acquired in the absence of nucleotides should be approximately equal (**Figure 3E**). These calculations are performed automatically by the software.

5.11.3. Obtain the output as an image plotting the data and a tabbed spreadsheet containing the raw spectra, subtracted spectra, spectra corrected for photobleaching, and the peak data for each file so that further analysis may be conducted.

6. Patch-clamp fluorometry experiments

6.1. Pull patch pipettes from thick-walled borosilicate glass capillaries to a resistance of 1.5 MΩ to 2.5 MΩ when filled with pipette solution. The composition of the pipette solution will vary depending on the protein under study.

6.2. Transfer a cover slip with transfected cells onto a cover glass-bottom 35 mm dish containing 2 mL bath solution and mount onto an inverted microscope equipped with a high NA, 60x water immersion objective. Perfuse the bath chamber (0.5 – 1 mL/min) with bath solution using a peristaltic pump. As for the pipette solution, the bath solution will vary depending on the protein under study.

6.3. Identify a cell expressing ANAP-labeled channels by looking for fluorescence at the cell membrane.

6.4. Fill a patch pipette with pipette solution. Apply gentle positive pressure to the pipette and place in the bath chamber. Press the pipette against the membrane of the cell and apply gentle suction to achieve a GΩ seal (**Figure 4A**).

6.5. Excise the patch by rapidly moving the pipette holder away from the patched cell (**Figure 4A**).

NOTE: Excising the patch in this will form an inside-out patch, with the cytosolic domains of the protein exposed to the perfusion system. If the location of the nucleotide binding site under study is not cytosolic, it will be necessary to use outside-out patches or whole cell recordings to perform PCF experiments.

6.6. Bring the tip of the patch pipette close to the tip of the perfusion system, and check that the patch is within the slit of the spectrometer mask (**Figure 4A**).

6.7. Apply TNP-ATP and image spectra as in steps 4.6-4.7, while simultaneously recording the ionic current response to nucleotide application.

NOTE: The pipette glass may introduce spatial aberrations and reflections in the acquired images. However, these aberrations will not affect the shape of the acquired spectra and reflected excitation light is easily separated from fluorescence using either the spectrograph or a long-pass emission filter.

6.8. Analyze the spectra. Spectra imaged from excised patches can exhibit over-subtraction of unbound TNP-ATP fluorescence due to the exclusion of TNP-ATP from the glass of the patch pipette (**Figure 4C-E**). This over-subtraction does not affect the ANAP emission spectrum and so can be ignored.

NOTE: As the fluorescence signal in excised patches will be lower than in unroofed membranes, it is important to use an exposure time which gives high enough signal-to-noise without bleaching ANAP too rapidly.

REPRESENTATIVE RESULTS:

Figure 2 depicts the basic experimental setup for measuring nucleotide binding to fluorescent proteins in unroofed membrane fragments obtained by sonication (**Figure 2A,B**). Two different approaches were used to obtain unroofed membranes, directly culturing cells on poly-L-lysine-coated cover slips or culturing cells on untreated glass and exposing them briefly to poly-L-lysine (0.1% in water) before unroofing. **Figure 2C** depicts a typical unroofed membrane fragment from an HEK-293T cell expressing K_{ATP} channels tagged with orange fluorescent protein (OFP). Unroofed membranes were virtually invisible in bright-field images and were identified by the fluorescence of tagged membrane proteins or by counter-staining with a membrane dye like octadecyl rhodamine B[13]. In addition to unroofed membranes, sonication of HEK-293T cells also produced partially unroofed cell fragments (**Figure 2D**)[10,17]. These fragments were visible in bright field. This might be the result of ruffled plasma membranes that are only poorly adherent to the cover glass. Alternatively, these fragments may contain vesicles and membranes from intracellular organelles. As such, it is preferable to acquire images only from "true" unroofed membranes, as labeled target protein associated with intracellular membranes may reflect intermediate stages of post-translational processing and assembly. Culturing cells on poly-L-lysine-coated glass is recommended as this resulted in a higher yield of "true" unroofed membranes upon sonication.

A microvolume perfusion system was applied to fluorescent nucleotides to minimize the quantities needed in a typical experiment (**Figure 2B**). Provided polyimide-coated glass tip was replaced with a hand-pulled borosilicate glass tip in our perfusion set up, which reduced the fluorescence background. To minimize nucleotide accumulation around the unroofed membranes being imaged, the entire bath chamber was slowly perfused with buffer. As such, we wished to measure the rate of solution change from our microvolume perfusion system and to verify that the we were able to achieve the intended ligand concentration in our region of interest, i.e., that the ligand from our perfusion system was not diluted directly into the bathing media before reaching the unroofed membrane. To control for these possibilities, the wash-in and wash-out of a 50 µM solution of tetramethylrhodamine-5-maleimide (TMRM) from our microvolume perfusion system directed at the surface of a cover glass-bottom dish perfused with water were measured (**Figure 2E**). Solution exchange kinetics were reproducible and well described by a single exponential decay with time constants less than 1 s for both wash-in and wash-out. Such solution exchange times limit our ability to measure kinetics of ligand binding and unbinding in our current setup. To verify that we were able to achieve the desired ligand concentration at the surface of the cover slip, we compared the fluorescence intensity of 50 µM TMRM delivered to the cover slip by our microvolume perfusion system to 50 µM TMRM in a still bath (**Figure 2F**). No difference in intensity was observed, verifying that appropriate ligand concentrations at the surface of the cover slip with our microvolume perfusion system can be achieved, even when the bath is perfused.

Figure 3A shows a spectral image obtained from ANAP-tagged K_{ATP} channels in an unroofed membrane from an HEK-239T cell exposed to 5 µM TNP-ATP. To obtain such images, emitted light from the unroofed membrane was directed through a spectrometer in series with a CCD

camera. The emitted fluorescence was diffracted off gratings and projected onto the camera chip, producing spectra. The resulting images retain spatial information in the *y* dimension, but the *x* dimension was replaced with wavelength. The region of interest (ROI), corresponding to the unroofed membrane is outlined in orange. Two regions of high intensity are evident in the image, corresponding to the peak emission of ANAP and TNP-ATP. This was best appreciated in the wavelength-by-wavelength-averaged (over the entire ROI) spectrum shown in **Figure 3B**. The peak ~470 nm corresponds to ANAP incorporated into K_{ATP}; the peak ~535 nm corresponds to TNP-ATP. To correct for background fluorescence and direct excitation of TNP-ATP in solution, a background region (**Figure 3A**, gray) was selected from each image. The averaged background spectrum is shown in **Figure 3B.** The final spectrum was obtained by subtracting the averaged background spectrum from the averaged ROI spectrum (**Figure 3C**).

ANAP is prone to photobleaching artefacts. **Figure 3D** shows the reduction in peak ANAP fluorescence after multiple exposures. The peak fluorescence from several exposures in the absence of TNP-ATP (or from washes in between concentrations of TNP-ATP) were fitted to a single-exponential decay and this was used to correct for photobleaching artefacts (**Figure 3E**). Performing concentration-response experiments from both low-to-high and high-to-low nucleotide concentrations is recommended. If bleaching correction does not introduce any additional artefacts, the results should be comparable[11].

Figure 5A shows representative spectral images from an unroofed membrane obtained from a cell expressing ANAP-tagged K_{ATP} channels in the absence and presence of TNP-ATP. The corrected spectra are shown in **Figure 5B**. Observing emission spectra, there was a clear separation between the donor and acceptor fluorescence emission. As some non-specific binding of TNP-ATP to naive plasma membranes from untransfected HEK-293T cells was observed, it is recommended to quantify FRET as a reduction in the donor (ANAP) fluorescence[10,11]. This peak was specific to the labeled receptor.

For ligands that induce a conformational change in their receptor, binding studies in isolation do not provide direct, mechanistically meaningful information about the ligand binding process[18]. The concentration-response relationship for ligand binding depends not only on the intrinsic binding affinity, but also the conformational change induced by ligand binding, and the inherent propensity of the receptor to change conformation in the absence of ligand. To better understand the processes underscoring ligand-receptor interactions, binding measurements can be paired with experiments that provide a readout of protein function. To this end, ion channels are an ideal model system, as their currents can be measured with sub-ms time resolution down to the single-molecule level using voltage clamp. Historically, paired current and fluorescence measurements have provided significant insights into the opening and closing (gating) of voltage- and ligand-gated ion channels[19-21]. Experiments have been conducted to simultaneously measure ionic currents and fluorescent cyclic nucleotide binding to various cyclic nucleotide-regulated channels[22-24]. These studies employed a ligand that increased its quantum yield upon binding. Fluorescence from unbound ligand in the volume of solution near the patch can be subtracted by imaging the patches using confocal microscopy[22,23]. In our studies, binding was measured using the reduction in ANAP fluorescence. As this signal is specific to the channel and FRET between ANAP and TNP-ATP is strongly distance dependent (half maximal at ~43 Å), contaminations of our signal were

avoided by non-specifically bound and unbound nucleotides.

Figure 4A shows a typical patch-clamp fluorometry (PCF) experiment. A high resistance (GΩ) seal was formed between a saline-filled borosilicate glass pipette (connected to a voltage clamp amplifier) and a cell expressing ANAP-tagged K_{ATP}. After the seal formation, the pipette was pulled away from the cell, allowing access to the intracellular nucleotide binding sites. The pipette was then positioned over the microscope objective, centered on the slit of the spectrometer mask and the outflow of the microvolume perfusion system (modified with a borosilicate glass tip) was brought close to the pipette (**Figure 4D**). Voltage was controlled and currents were measured from the channels in the patch. Representative currents and spectra from ANAP-tagged K_{ATP} channels are shown in Figure 4B, color coded to match the spectra to the currents. Emission spectra were corrected for background and bleaching as for unroofed membranes.

FIGURE AND TABLE LEGENDS:

Figure 1: ANAP and TNP-ATP make a suitable FRET pair. (**A**) Structures of ANAP and TNP-ATP. The fluorescent moieties are highlighted. (**B**) Absorbance and fluorescence emission spectra of ANAP and TNP-ATP. Overlap between ANAP emission and TNP-ATP absorbance is required for FRET. Adapted from Puljung et al. (published under the Creative Commons Attribution License, https://creativecommons.org/licenses/by/4.0/)[10].

Figure 2: Measuring nucleotide binding in unroofed plasma membranes. (**A**) Schematic for the preparation of unroofed plasma membranes from adherent cells expressing a fluorescent membrane protein. Instructions are provided for cells grown on poly-L-lysine-coated or untreated cover slips. (**B**) Experimental setup for measuring nucleotide binding in unroofed membranes. (**C**) Bright field and fluorescent images of a completely unroofed plasma membrane derived from a cell expressing orange fluorescent protein (OFP) tagged K_{ATP} channels. The asterisk marks the position of the membrane, which is nearly invisible in the bright-field image. OFP was excited with a broad 565 nm LED through a 531/40 nm band-pass filter and 562 nm edge dichroic and emitted light was collected through a 593/40 nm band-pass filter. (**D**) Bright field and fluorescent images of a partially unroofed membrane fragment derived from a cell expressing orange fluorescent protein (OFP) tagged K_{ATP} channels. (**E**) Solution exchange time course acquired using the setup described in B. Five technical replicates are shown. The microvolume perfusion system was loaded with 50 µM tetramethylrhodamine-5-maleimide (TMRM). The bath was perfused with water at a rate of ~0.5 mL/min. Data from the wash-on (increasing fluorescence) and wash-out (decreasing fluorescence) time courses were fit with a single exponential decay of the form $F = A^*\exp(-x/\tau) + y_0$. The time constant ($\tau$) for wash-in was ~0.6 s. The time constant for wash-out was ~1.0 s. TMRM was excited with a broad 565 nm LED through a 540/25 nm band-pass filter and 565 nm edge dichroic and emitted light was collected through a 605/55 nm band-pass filter. (**F**) Comparison of the fluorescence intensity of a 50 µM solution of TMRM applied using the microvolume perfusion system as in B and a still bath containing 50 µM TMRM.

Figure 3: Background subtraction and bleaching correction. (**A**) Spectral image (spatial information in the *y* dimension, wavelength in the *x* dimension) of an unroofed plasma membrane from a cell expressing ANAP-labeled K_{ATP} channels. 5 µM TNP-ATP was applied

using the setup described in Figure 2B. The orange box denotes the region of interest (ROI), corresponding to the unroofed membrane. The gray box denotes the background region used for correcting the spectrum. (**B**) Emission spectra derived from wavelength-by-wavelength averages of the ROI and background regions in A. (**C**) Spectrum derived by subtracting the averaged background spectrum from the averaged ROI spectrum in B. The 5 nm window around the ANAP peak used to determine the average intensity is shown as a gray shaded area. (**D**) Spectra acquired from six consecutive 10-s exposures of an unroofed plasma membrane from a cell expressing ANAP-labeled K_{ATP} channels. Note the decrement in fluorescence resulting from photobleaching. The inset shows the normalized peak fluorescence fit with a single exponential decay of the form $F/F_{max} = A*\exp(-t/\tau) + (1-A)$. The symbols in the inset are color-coded to match the spectra. (**E**) The same spectra as in D corrected for photobleaching. The inset shows the normalized peak fluorescence from D as open circles, with the corrected peak fluorescence shown using filled circles.

Figure 4: Simultaneous measurements of nucleotide binding and channel currents using patch-clamp fluorometry (PCF). (**A**) Schematic showing the experimental setup for measuring nucleotide binding and ionic currents. (**B**) Example currents (left) and spectra (right) acquired from a membrane patch excised from a cell expressing ANAP-labeled K_{ATP} channels. Currents were recorded at a holding potential of -60 mV, digitized at 20 kHz, and filtered at 5 kHz. The gray shaded area corresponds to the wavelength range from which ANAP intensity was quantified. Adapted from Usher et al. (published under the Creative Commons Attribution License, https://creativecommons.org/licenses/by/4.0/)[11]. (**C**) Spectrum acquired from a membrane patch excised from a cell expressing ANAP-labeled K_{ATP} channels exposed to 1 mM TNP-ATP. Note the negative peak corresponding to the wavelength range over which TNP-ATP fluorescence is observed. The gray shaded area denotes the wavelength range used to quantify ANAP fluorescence as in B. Adapted from Usher et al. (published under the Creative Commons Attribution License, https://creativecommons.org/licenses/by/4.0/)[11]. (**D**) Bright field and fluorescent images of a patch pipette exposed to 1 mM TNP-ATP. The asterisk marks the tip of the pipette. (**E**) Spectral image of the same patch pipette in 1 mM TNP-ATP. The asterisk marks the position of the pipette.

Figure 5: TNP-ATP binding to ANAP-labeled K_{ATP} channels. (**A**) Spectral images of an unroofed plasma membrane from a cell expressing ANAP-labeled K_{ATP} channels in the absence of TNP-ATP or in the presence of 50 µM or 1 mM TNP-ATP. Intensities are shown as a heat map. (**B**) Wavelength-by-wavelength-averaged spectra from the images in A showing quenching of ANAP fluorescence by TNP-ATP. The shaded areas represent two different band-pass filters that can be used to measure ANAP quenching if a spectrometer is not available.

Figure 6: Quenching of ANAP-labeled K_{ATP} channels by TNP-ATP in unroofed membranes and PCF. Overlay of data from Usher et al. (published under the Creative Commons Attribution License, https://creativecommons.org/licenses/by/4.0/)[11]. Data were fit to the Hill equation: $F / F_{max} = E_{max} + (1 - E_{max}) / (1+10^{(EC50 - [TNP\text{-}ATP])*h})$. F is the measured fluorescence, F_{max} is the maximal fluorescence in the absence of nucleotide, E_{max} is the maximal quenching at saturating nucleotide concentrations, and h is the Hill slope. *EC50*, (the nucleotide concentration at which quenching is half maximal) and [*TNP-ATP*] are log values. Unroofed membranes: *EC50* = -4.59 (25.7 µM), h = 0.82, E_{max} = 0.93. PCF: *EC50* = -4.11 (77.6 µM), h = 0.87, E_{max} = 1.00.

DISCUSSION:

We have developed a method to measure adenine nucleotide binding in real time to intact membrane proteins. Our method builds on several other established techniques including labeling of proteins with ANAP using amber stop codon suppression[12], cell unroofing[14], and voltage-clamp fluorometry/PCF[19-25]. The synthesis of these approaches allows for measurement of nucleotide binding with high spatial and temporal resolution. Indeed, in our previous work, we were able to distinguish between different binding sites on the same protein complex using this approach[10,11]. Importantly, this technique can be directly applied to small amounts of protein in a cellular environment under conditions that preserve protein function. Using our binding method in conjunction with direct, electrophysiological readout of ion channel currents allows us to obtain rich insights into the molecular underpinnings of channel gating[11].

As spectrometers are a non-standard piece of laboratory equipment, ANAP intensity can also be monitored in relative isolation using band-pass filters. **Figure 5B** depicts the spectral properties of two such filters. The 470/10 nm band-pass filter effectively screens out the fluorescence signal from TNP-ATP and overlaps well with the peak ANAP fluorescence. However, the peak transmittance of this filter is only around 50%, which may make it difficult to obtain good signals from dim membranes (or in excised membrane patches under voltage clamp). Another option is a 460/60 nm band-pass filter. There is slightly more overlap between the 460/60 nm filter and the foot of the TNP-ATP emission peak compared to the 470/10 nm filter. However, the 460/60 nm band-pass has a transmittance of 90-95% over a broad range of the ANAP peak, which would be expected to boost the fluorescence emission signal.

ANAP is an environmentally sensitive fluorophore[12,26,27]. The peak emission and quantum yield vary depending on the site of incorporation on the protein of interest and may change as the protein changes conformation. Such changes would be immediately evident from emission spectra but would not be as obvious when ANAP intensity is measured using filters. In any case, appropriate controls are required to demonstrate that the fluorescence signal does not vary because of changes in the local environment around ANAP subsequent to the nucleotide binding. Control experiments with unlabeled nucleotides can help verify that any changes in ANAP intensity are the result of FRET between ANAP and TNP-nucleotides. TNP-nucleotides can bind non-specifically to the membranes derived from untransfected cells (either to the plasma membrane or to native membrane proteins)[10]. We quantify binding as a decrement in the donor fluorescence, as this signal is specific to the labeled channel. However, we recommend performing additional control experiments for each agonist/receptor pair, for example mutating the nucleotide binding site if known, to verify that the change in donor fluorescence is really the result of direct binding to the labeled receptor[11]. Finally, working with constructs that contain a fluorescent protein tag in addition to the ANAP label is recommended. This helps to differentiate labeled receptor fluorescence from background/autofluorescence. Background fluorescence can be distinguished from ANAP by the peak and shape of emission spectra[10], but such determinations can be very difficult when only filter sets are used. Additionally, cells and unroofed membranes expressing fluorescent receptors can be identified using the fluorescent protein tag without having to excite ANAP and risk excessive photobleaching.

In many of our PCF records, we observed a strong negative peak in our spectra at high TNP-ATP concentrations (**Figure 4C**). This negative peak is an artefact of our background subtraction protocol. **Figure 4D** shows bright-field and fluorescent images of a patch pipette exposed to 1 mM TNP-ATP. A shadow at the pipette tip is evident, resulting from exclusion of TNP-ATP from the volume of the pipette walls, which is most evident within the plane of focus. The spectral image in **Figure 4E** shows a dark band, corresponding to this shadow. When a region above or below this dark band is used for background subtraction, it produces a negative peak. Importantly, this peak occurred over a wavelength range corresponding to TNP-ATP emission and did not affect our measurements of ANAP quenching.

The major limitation of our experiments was in obtaining adequate plasma membrane expression of ANAP-tagged constructs to measure fluorescence. It was generally easier to acquire high quality spectra from unroofed membranes than in PCF, due to their larger size and our ability to quickly scan an entire dish of unroofed membranes, unlike in PCF where patches can only be obtained one at a time. In our experiments, the data from unroofed membranes and PCF experiments were similar but not equivalent (**Figure 6**)[11]. However, there is no a priori reason why this should be a universal observation as proteins in a patch pipette may be in a different functional state than those in unroofed membranes.

Here, attempts have been made to maximize expression of our ANAP-tagged constructs, in particular lowering the cell culture temperature to 33 °C[10,11,16]. In our experience, attempting to identify sites in the protein at which ANAP would be a conservative substitution did not consistently result in constructs that expressed well. We had more success systematically scanning entire protein regions for ANAP incorporation sites and screening candidates for surface expression[10]. The ANAP labeling system also works in *Xenopus laevis* oocytes, which allows for much larger membrane patches to be excised, thus increasing signal to noise[26-28].

Whereas larger levels of expression are expected to result in brighter signals, the minimum number of channels required to measure fluorescence depends on several factors, including the brightness of the fluorophore, the degree of photobleaching, the intensity of the excitation light, and the plane of focus. In theory, estimates could be made by correlating the fluorescence intensity and the channel current as has been shown previously[28,29]. However, the reliability of such estimates requires some knowledge of the single-channel conductance and the channel's open probability. In addition to the factors listed above, the fluorescence signal will also be affected by channels associated with vesicles or sections of the plasma membrane stuck to the pipette glass that are not under voltage clamp.

This method is readily adapted to the study of other nucleotide-sensitive ion channels. CFTR is structurally similar to the accessory sulfonylurea receptor subunit of K_{ATP}[30,31]. Like K_{ATP} CFTR gating is controlled by nucleotide binding, making it an obvious future target of our method[7]. Purinergic P2X receptors are ion channels gated by extracellular ATP[9]. TNP-ATP acts as an antagonist for P2X receptors[32,33]. Therefore, it will not be useful for studying P2X activation, although it may be used in competition assays with P2X agonists. Alternatively, other fluorescent ATP derivatives with sufficient spectral overlap with ANAP emission may be used to study activation. Alexa-647-ATP is a fluorescent P2X agonist[34]. The calculated R_0 between Alexa-647 and ANAP is ~85 Å, which means that direct binding to P2X should result in

substantial quenching of ANAP incorporated into the channel. However, such a long R_0 will also result in quenching from Alexa-647-ATP bound to neighboring subunits and increases the likelihood that non-specific nucleotide binding will result in FRET. As the ligand binding site in P2X receptors is extracellular, binding measurements would be performed on intact cells, in whole-cell voltage clamp, or in outside-out membrane patches. Our method can also be extended to study binding and activation of electrogenic and non-electrogenic transporters and pumps that depend on ATP for their reaction cycle as well as G protein coupled P2Y receptors. Finally, even though we have developed this method to measure adenine nucleotide binding (TNP-ATP, TNP-ADP, TNP-AMP), the same approach can be used to study binding to virtually any receptor for which a suitable, fluorescent ligand has been identified.

ACKNOWLEDGMENTS:

We wish to thank Raul Terron Exposito for excellent technical assistance. This work was funded by the Biotechnology and Biological Sciences Research Council (BB/R002517/1; MCP and FMA) and the Wellcome Trust (203731/Z/16/A; SGU)

DISCLOSURES:

The authors declare no conflicts of interest.

REFERENCES:

1 Garcia, M. L., Kaczorowski, G. J. Ion channels find a pathway for therapeutic success. *Proceedings of the National Academy of Sciences of the United States of America.* **113** (20), 5472-5474 (2016).

2 Hauser, A. S., Attwood, M. M., Rask-Andersen, M., Schioth, H. B., Gloriam, D. E. Trends in GPCR drug discovery: new agents, targets and indications. *Nature Reviews Drug Discovery.* **16** (12), 829-842 (2017).

3 Lakowicz, J. R. *Principles of fluorescence spectroscopy*. 3rd edn, Springer. (2006).

4 Higgins, C. F., Linton, K. J. The ATP switch model for ABC transporters. *Nature Structural & Molecular Biology.* **11** (10), 918-926 (2004).

5 Toyoshima, C., Cornelius, F. New crystal structures of PII-type ATPases: excitement continues. *Current Opinion in Structural Biology.* **23** (4), 507-514 (2013).

6 Craven, K. B., Zagotta, W. N. CNG and HCN channels: two peas, one pod. *Annual Review of Physiology.* **68**, 375-401 (2006).

7 Csanady, L., Vergani, P., Gadsby, D. C. Strict coupling between CFTR's catalytic cycle and gating of its Cl- ion pore revealed by distributions of open channel burst durations. *Proceedings of the National Academy of Sciences of the United States of America.* **107** (3), 1241-1246 (2010).

8 Vedovato, N., Ashcroft, F. M., Puljung, M. C. The Nucleotide-Binding Sites of SUR1: A Mechanistic Model. *Biophysical Journal.* **109** (12), 2452-2460 (2015).

9 Burnstock, G. Introduction to the Special Issue on Purinergic Receptors. *Advances in Experimental Medicine and Biology.* **1051**, 1-6 (2017).

10 Puljung, M., Vedovato, N., Usher, S., Ashcroft, F. Activation mechanism of ATP-sensitive K(+) channels explored with real-time nucleotide binding. *Elife.* **8**, e41103 (2019).

11 Usher, S. G., Ashcroft, F. M., Puljung, M. C. Nucleotide inhibition of the pancreatic ATP-sensitive K+ channel explored with patch-clamp fluorometry. *Elife.* **9**, e52775 (2020).

12 Chatterjee, A., Guo, J., Lee, H. S., Schultz, P. G. A genetically encoded fluorescent probe in mammalian cells. *Journal of the American Chemical Society.* **135** (34), 12540-12543 (2013).

13 Gordon, S. E., Senning, E. N., Aman, T. K., Zagotta, W. N. Transition metal ion FRET to measure short-range distances at the intracellular surface of the plasma membrane. *Journal of General Physiology.* **147** (2), 189-200 (2016).
14 Heuser, J. The production of 'cell cortices' for light and electron microscopy. *Traffic.* **1** (7), 545-552 (2000).
15 Schmied, W. H., Elsasser, S. J., Uttamapinant, C., Chin, J. W. Efficient multisite unnatural amino acid incorporation in mammalian cells via optimized pyrrolysyl tRNA synthetase/tRNA expression and engineered eRF1. *Journal of the American Chemical Society.* **136** (44), 15577-15583 (2014).
16 Lin, C. Y. et al. Enhancing Protein Expression in HEK-293 Cells by Lowering Culture Temperature. *PloS One.* **10** (4), e0123562 (2015).
17 Usukura, J. et al. Use of the unroofing technique for atomic force microscopic imaging of the intra-cellular cytoskeleton under aqueous conditions. *Journal of Electron Microscopy.* **61** (5), 321-326 (2012).
18 Colquhoun, D. Binding, gating, affinity and efficacy: the interpretation of structure-activity relationships for agonists and of the effects of mutating receptors. *British Journal of Pharmacology.* **125** (5), 924-947 (1998).
19 Mannuzzu, L. M., Moronne, M. M., Isacoff, E. Y. Direct physical measure of conformational rearrangement underlying potassium channel gating. *Science.* **271** (5246), 213-216 (1996).
20 Zheng, J., Zagotta, W. N. Gating rearrangements in cyclic nucleotide-gated channels revealed by patch-clamp fluorometry. *Neuron.* **28** (2), 369-374 (2000).
21 Zheng, J., Zagotta, W. N. Patch-clamp fluorometry recording of conformational rearrangements of ion channels. *Science's STKE.* **2003** (176), PL7 (2003).
22 Biskup, C. et al. Relating ligand binding to activation gating in CNGA2 channels. *Nature.* **446** (7134), 440-443 (2007).
23 Kusch, J. et al. Interdependence of receptor activation and ligand binding in HCN2 pacemaker channels. *Neuron.* **67** (1), 75-85 (2010).
24 Wu, S. et al. State-dependent cAMP binding to functioning HCN channels studied by patch-clamp fluorometry. *Biophysical Journal.* **100** (5), 1226-1232 (2011).
25 Cha, A., Bezanilla, F. Characterizing voltage-dependent conformational changes in the Shaker K+ channel with fluorescence. *Neuron.* **19** (5), 1127-1140 (1997).
26 Kalstrup, T., Blunck, R. Dynamics of internal pore opening in K(V) channels probed by a fluorescent unnatural amino acid. *Proceedings of the National Academy of Sciences of the United States of America.* **110** (20), 8272-8277 (2013).
27 Kalstrup, T., Blunck, R. S4-S5 linker movement during activation and inactivation in voltage-gated K(+) channels. *Proceedings of the National Academy of Sciences of the United States of America.* **115** (29), E6751-E6759 (2018).
28 Dai, G., Aman, T. K., DiMaio, F., Zagotta, W. N. The HCN channel voltage sensor undergoes a large downward motion during hyperpolarization. *Nature Structural & Molecular Biology.* **26** (8), 686-694 (2019).
29 Liu, C. et al. Patch-clamp fluorometry-based channel counting to determine HCN channel conductance. *Journal of General Physiology.* **148** (1), 65-76 (2016).
30 Hwang, T. C. et al. Structural mechanisms of CFTR function and dysfunction. *Journal of General Physiology.* **150** (4), 539-570 (2018).
31 Puljung, M. C. Cryo-electron microscopy structures and progress toward a dynamic understanding of KATP channels. *Journal of General Physiology.* **150** (5), 653-669 (2018).

32 Kasuya, G. et al. Structural insights into the competitive inhibition of the ATP-gated P2X receptor channel. *Nature Communications.* **8** (1), 876 (2017).
33 Virginio, C., Robertson, G., Surprenant, A., North, R. A. Trinitrophenyl-substituted nucleotides are potent antagonists selective for P2X1, P2X3, and heteromeric P2X2/3 receptors. *Molecular Pharmacology.* **53** (6), 969-973 (1998).
34 Bhargava, Y., Nicke, A., Rettinger, J. Validation of Alexa-647-ATP as a powerful tool to study P2X receptor ligand binding and desensitization. *Biochemical and Biophysical Research Communications.* **438** (2), 295-300 (2013).

Figure 1

Click here to access/download;Figure;Figure 1_Usher_JoVE61401.pdf

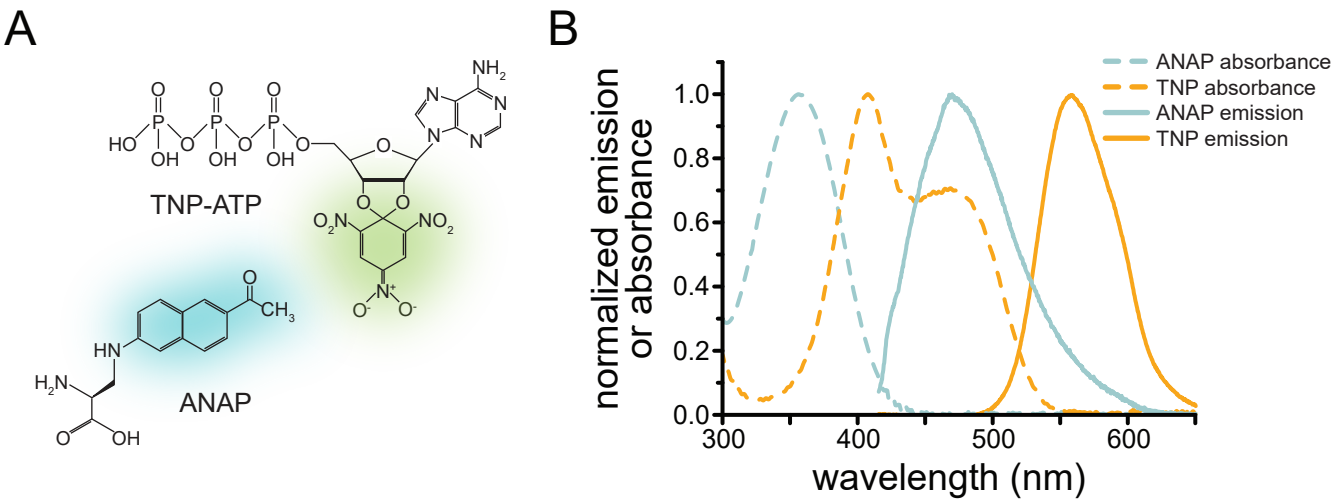

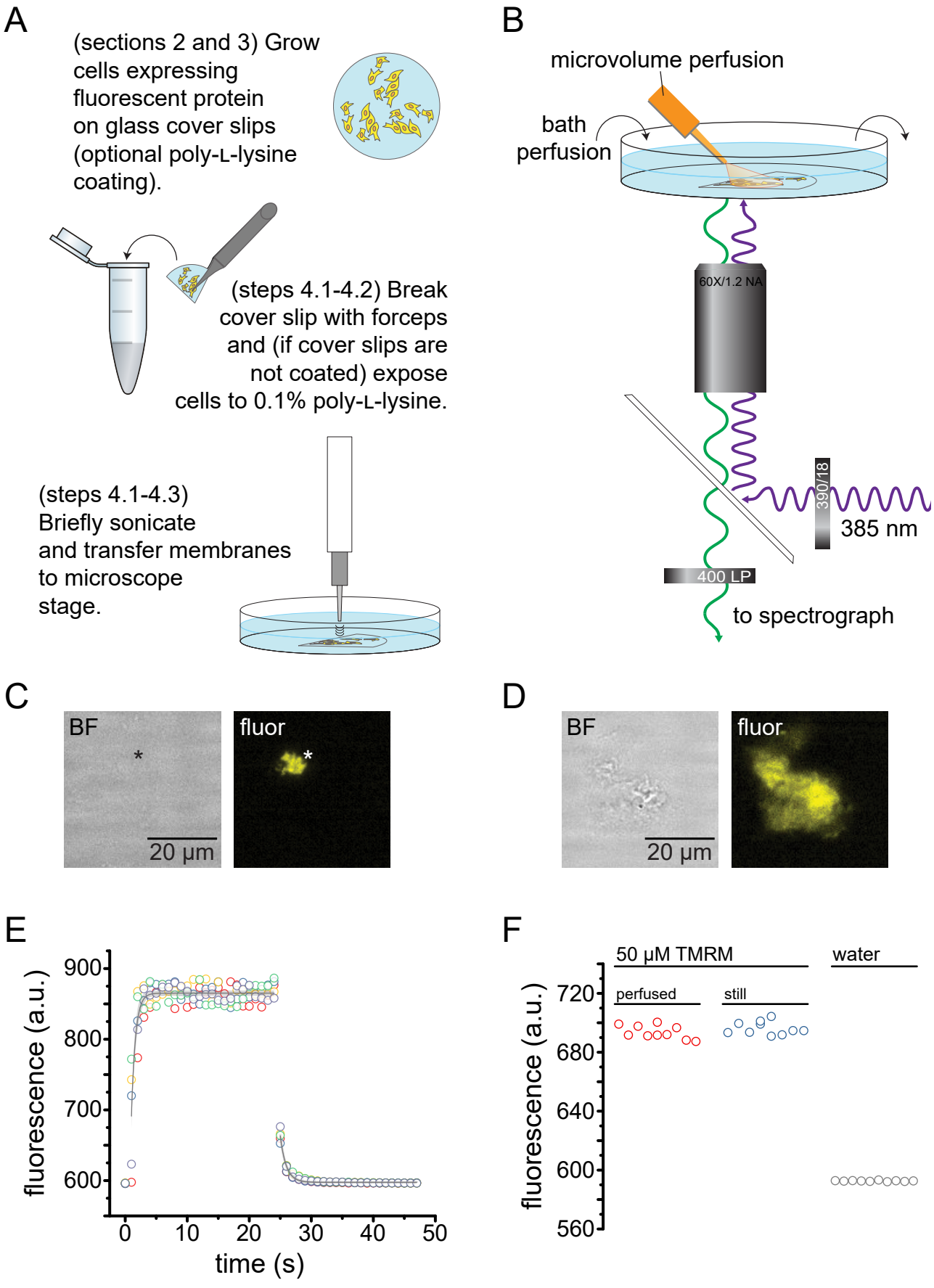

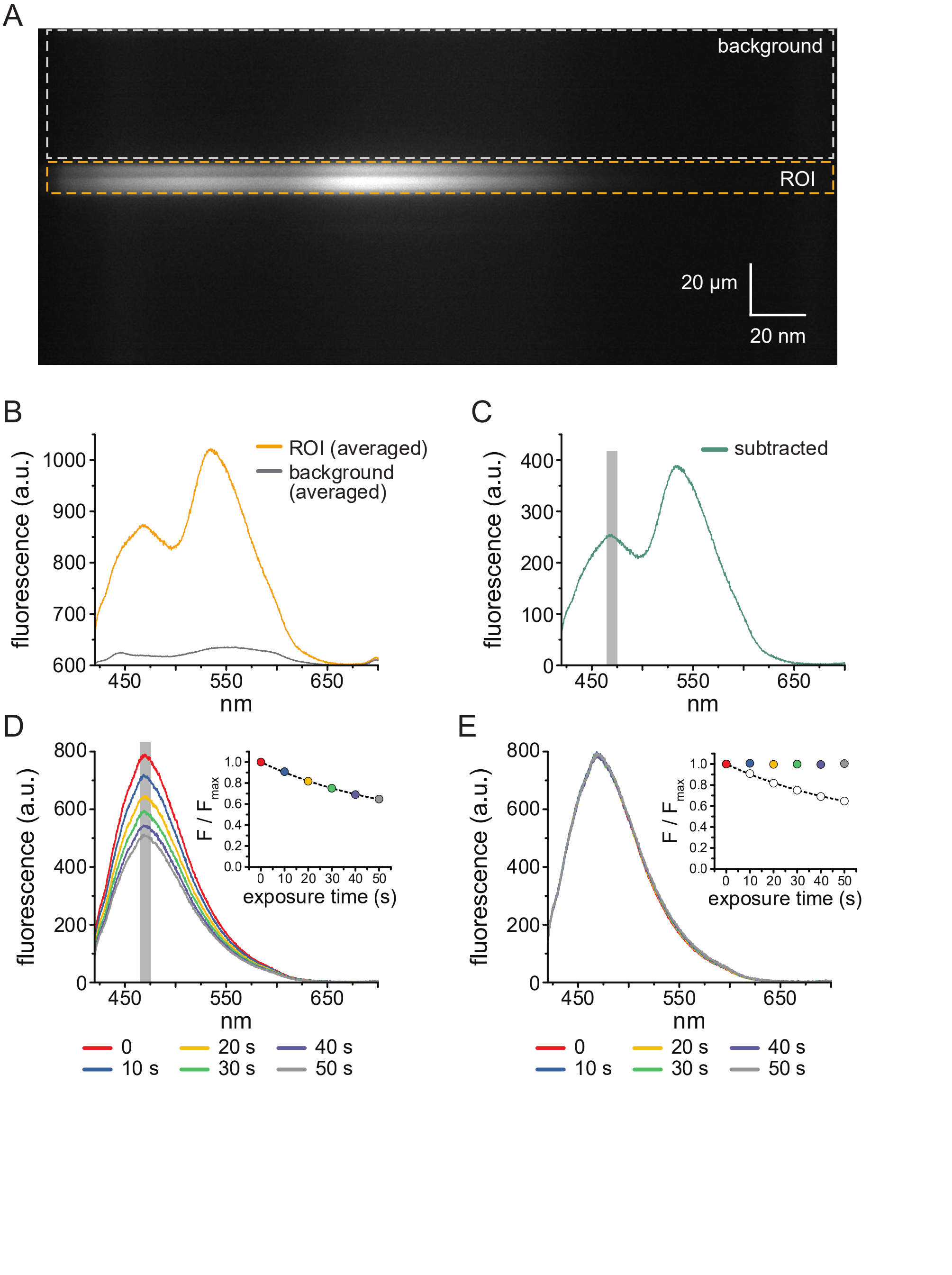

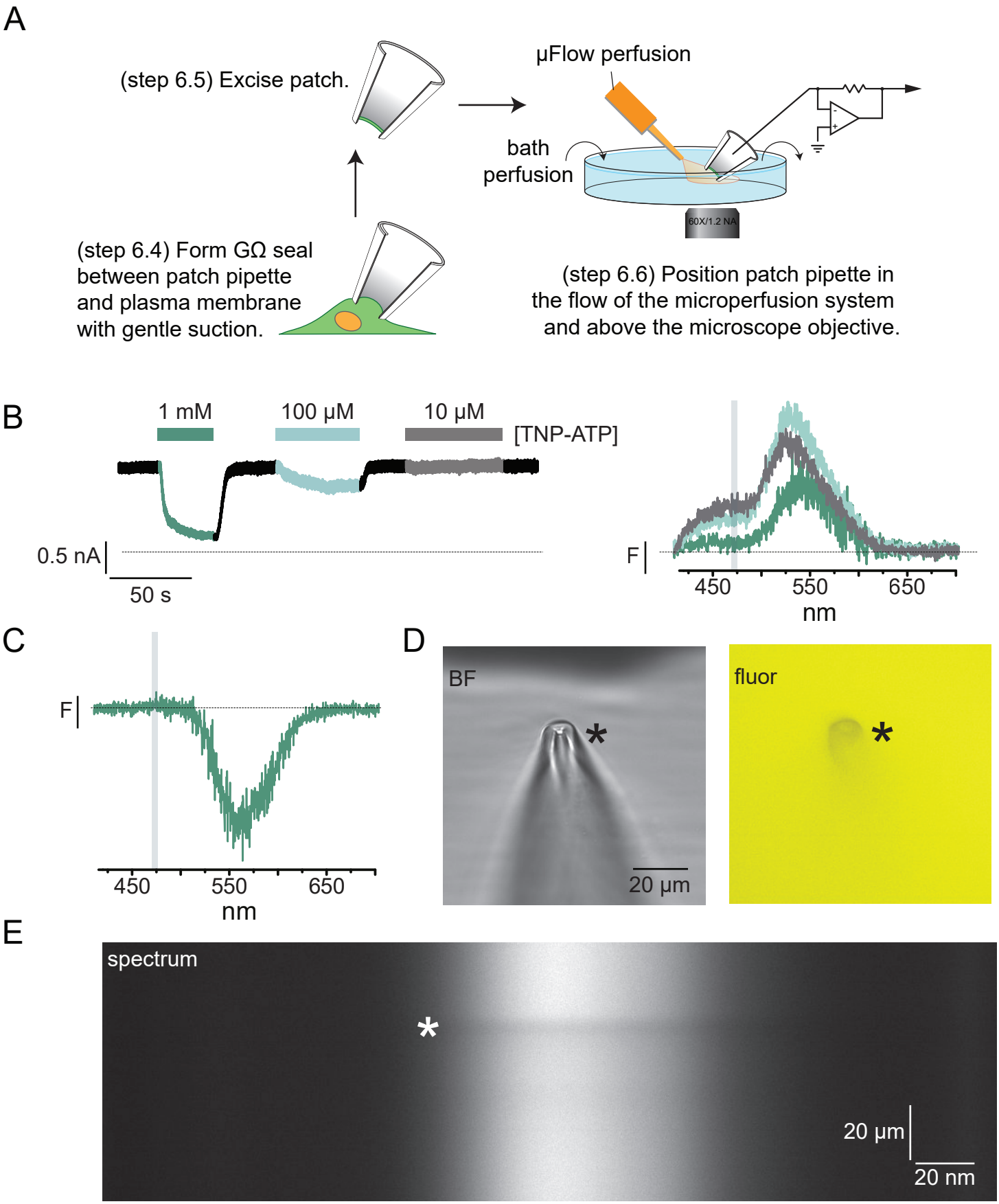

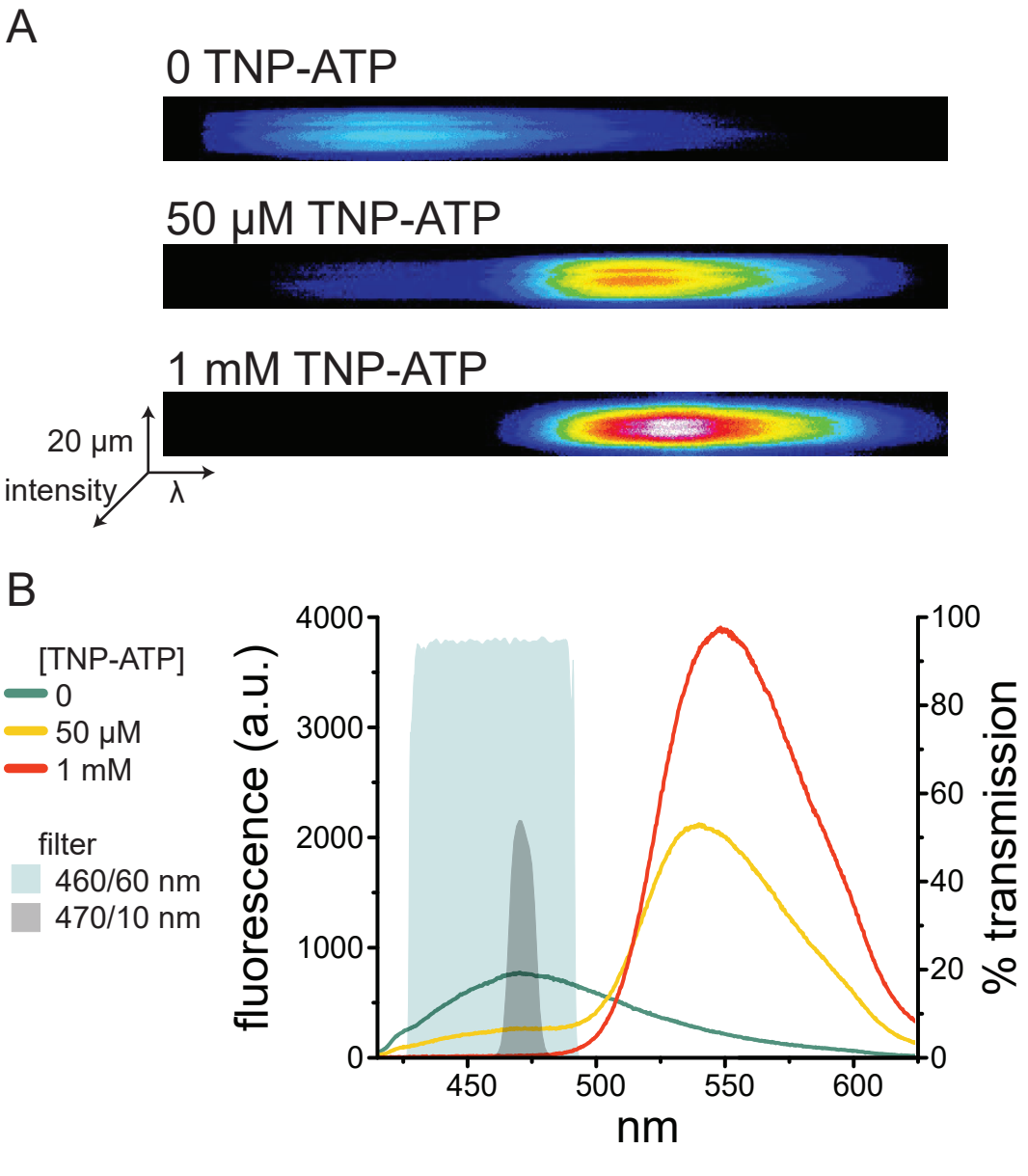

Figure 6

Click here to access/download;Figure;Figure 6_Usher_JoVE61401.pdf

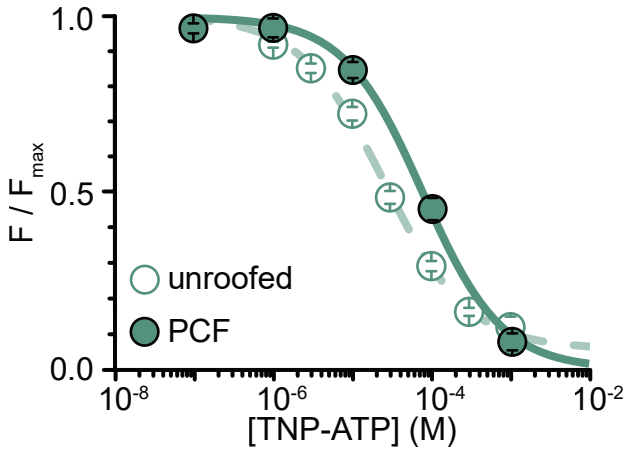

Name of Material/ Equipment	Company	Catalog Number
0.1% w/v poly-L-lysine	Sigma-Aldrich	P8920
30 mm borosilicate cover glass slips	VWR	631-0174
35 mm cover glass bottom dish	WPI	FD35-PDL-100
35 mm non-treated sterile dishes	CytoOne	CC7672-3340
390/18 nm band-pass excitation filter	ThorLabs	MF390-18
400 nm long-pass emission filter	ThorLabs	FEL0400
416 nm edge dichroic	ThorLabs	MD416
460/60 nm band-pass emission filter	ThorLabs	MF460-60
470/10 nm band-pass emission filter	ThorLabs	FB470-10
4-Wavelength High-Power LED Head	ThorLabs	LED4D245
531/40 band-pass excitation filter	Brightline	FF01-531/40-25
540/25 nm band-pass excitation filter	Chroma	D540/25X
562 nm edge dichroic	Semrock	FF562-Di03
565 nm edge dichroic	Chroma	565DC
593/40 nm band-pass excitation filter	Brightline	FF01-387/11-25
605/55 nm band-pass emission filter	Chroma	D605/55M
60x water immersion objective (1.4 NA)	Nikon	MRD07602
ANAP-TFA	AsisChem	ASIS-0014
Axopatch 200B amplifier	Molecular Devices	Axopatch 200B-2
Digidata 1440A digitizer	Molecular Devices	Digidata 1440A
Dulbecco’s Modified Eagle Medium (DMEM)	Gibco	31966021
Foetal bovine serum (FBS)	Gibco	10500-064
Four-Channel LED Driver	ThorLabs	DC4100
HEK293T cells	ATTC	CRL-3216
IsoPlane-160 Imaging Spectrometer	Princeton Instruments	IsoPlane-160
Lightfield 5.20.1507	Princeton Instruments	
Matlab	Mathworks	
Microvolume perfusion system	ALA Scientific Instruments	ALA µFlow-8
Nikon Eclipse TE2000-U inverted microscope	Nikon	
pANAP expression plasmid	Addgene	Plasmid #48696
pClamp 10.6.2	Molecular Devices	
Penicillin/Streptomycin	Gibco	15140-122

peRF1-E55D	Chin Lab (MRC Laboratory of	Jason Chin: DOI: 10.1021/ja5069728
Phosphate buffered saline (PBS)	Gibco	14040-091
PIXIS 400BR_eXcelon Camera	Princeton Instruments	PIXIS: 400BR_eXcelon
Probe sonicator	Sonics & Materials	VC-50
Python 3.8.1	Python Software Foundation	
REGLO digital peristaltic pump	Ismatec	ISM 832
T75 tissue-culture treated flask	StarLab	CC7682-4875
Tetramethylrhodamine-5-maleimide	Sigma-Aldrich	94506
Thick-walled borosilicate glass capillaries	Harvard Apparatus	GC150F-15
TNP-ATP	Jena Bioscience	NU-221L
TransIT-LT1	Mirus Bio	MIR 2300
TrypLE select (tryosin)	Gibco	12563-011
UltraPure distilled water	Invitrogen	10977-035

	Comments/Description
For ANAP excitation	
For imaging ANAP spectra	
For imaging ANAP spectra	
Suggested wide band-pass filter for imaging ANAP fluorescence (Figure 4B)	
Suggested narrow band-pass filter for imaging ANAP fluorescence (Figure 4B)	
385/490/565/625 nm LEDs	
For orange fluorescent protein (OFP) excitation	
For tetramethylrhodamine-5-maleimide (TMRM) excitation	
For imaging OFP fluorescence	
For imaging TMRM fluorescence	
For imaging OFP fluorescence	
For imaging TMRM fluorescence	
Reconstituted in 30 mM NaOH to a final concentration of 1 mM	
Used between passages 5-30	
Acquisition software for images and spectra	
For data analysis	
For TNP-ATP perfusion	
Encodes tRNA/tRNA synthetase pair for expression of ANAP-tagged protein	
Recording and analysing currents	

Encodes dominant-negative eukaryotic ribosomal release factor

For unroofing
For data analysis
For bath perfusion

Delivered at 10 mM in water
Lipopolyplex transfection reagent

DEPARTMENT OF PHYSIOLOGY, ANATOMY AND GENETICS

Michael C. Puljung, Ph.D.
Sherrington Building, Parks Road, Oxford OX1 3PT
Tel: +44(0)1865 285891
michael.puljung@dpag.ox.ac.uk

Benjamin Werth, BS
Science Editor, *JoVE*
1 Alewife Center, Suite 200
Cambridge, MA 02140

6 May 2020

Dear Benjamin,

I am pleased to resubmit our manuscript “Measuring nucleotide binding to intact, functional membrane proteins in real time” (JoVE61401) on behalf of Samuel Usher, Frances Ashcroft, and myself for consideration as an Article in *JoVE*. I apologize for the delay in making our revisions. We have had to close the laboratory due to the spread of SARS-Cov-2.

We thank you and the reviewers for the helpful suggestions. In response to their suggestions we have amended the text and figures (as outlined in our specific responses below) and have included an additional Figure 6. We feel that these changes have improved the readability of our work and will greatly aid future experimenters in following our protocol. Please note that we have also reworded the manuscript title to make its meaning less ambiguous. We hope you will find this revised version of our manuscript acceptable for publication in *JoVE.*

As previously noted, I will be relocating to Trinity College in Connecticut in July. Therefore, I will be unavailable for a period of time after June for filming. Sam Usher would be more than happy to be filmed in the event of my absence. Of course, we understand that the ability to film this work will be greatly impacted by the current pandemic.

Thank you again for considering our manuscript for publication. I look forward to hearing your response.

Yours sincerely,

Michael C. Puljung, Ph.D.
Departmental Lecturer
Department of Physiology, Anatomy and Genetics
University of Oxford

Editorial Comments:

• *Please take this opportunity to thoroughly proofread the manuscript to ensure that there are no spelling or grammatical errors.*

• ***Protocol Detail:*** *Please note that your protocol will be used to generate the script for the video, and must contain everything that you would like shown in the video.* ***Please add more specific details (e.g. button clicks for software actions, numerical values for settings, etc) to your protocol steps.*** *There should be enough detail in each step to supplement the actions seen in the video so that viewers can easily replicate the protocol. (Hz).*

Many of the specific clicks are specific to the proprietary software that came with our camera/spectrograph and are not generalizable to other users. Therefore, we mention changes in settings in lieu of specific clicks.

1) 4.2.1: mention sonication amplitude (watts) and frequency.

We now include more detail about the sonicator in lines 128-133, including a note on adjustments.

2) Section 5: Please mention all button clicks and software selections in order to enable filming. What kind of software is used? Is it GUI based? Please list it in the table of materials.

The software is now listed in the table of materials. Acquisition software for images and ionic currents are both GUI-based and proprietary. As stated above, we mention settings rather than specific clicks, as these software packages are not generalizable to all users.

• ***Discussion:*** *JoVE articles are focused on the methods and the protocol, thus the discussion should be similarly focused. Please ensure that the discussion covers the following in detail and in paragraph form (3-6 paragraphs): 1) modifications and troubleshooting, 2) limitations of the technique, 3) significance with respect to existing methods, 4) future applications and 5) critical steps within the protocol.*

• ***Figures:***
1) Please list figures in the order that they are reference. Currently fig 2 is referenced first.

Figure 1 is referenced first in the introduction (lines 70-71). We have deleted a premature reference to Figure 4.

• ***References:*** *Please spell out journal names.*

We have made this change.

• ***Commercial Language:*** *JoVE is unable to publish manuscripts containing commercial sounding language, including trademark or registered trademark symbols (TM/R) and the mention of company brand names before an instrument or reagent. Examples of commercial sounding language in your manuscript are TransIT-LT1*

1) Please use MS Word's find function (Ctrl+F), to locate and replace all commercial sounding language in your manuscript with generic names that are not company-specific. All commercial products should be sufficiently referenced in the table of materials/reagents. You may use the generic term followed by "(see table of materials)" to draw the readers' attention to specific commercial names.

We have replaced references to TransIT-LT1 (line 115) with the generic term. We have read through the remainder of the document to remove commercial language and have placed all such language in the materials list.

• *If your figures and tables are original and not published previously or you have already obtained figure permissions, please ignore this comment. If you are re-using figures from a previous publication, you must obtain explicit permission to re-use the figure from the previous publisher (this can be in the form of a letter from an editor or a link to the editorial policies that allows you to re-publish the figure). Please upload the text of the re-print permission (may be copied and pasted from an email/website) as a Word document to the Editorial Manager site in the "Supplemental files (as requested by JoVE)" section. Please also cite the figure appropriately in the figure legend, i.e. "This figure has been modified from [citation]."*

We have obtained permission from *eLIFE* to adapt our figures and have included the permission with this resubmission. The originals were published under the Creative Commons Attribution License and are free to use without permission.

Comments from Peer-Reviewers:

Reviewer #1:
Manuscript Summary:
The authors describe a very useful technique bearing the potential to be applied in a wide variety of different membrane proteins. Overall the protocol is described in such a way that it can be followed easily step by step, even including some alternatives for different kinds of setups. However, I want to mention some minor points, which can be described more

thoroughly.

Major Concerns:
none

Minor Concerns:
1. Regarding 4.2.2. What is the reason for dipping not pre-coated cover slips into the poly-L-lysine solution 30 sec before sonicating? Is it expected that it affects cell adherence is such a short amount of time? Maybe the authors can comment a bit more about that option.

It has been previously shown (reference 13) that perfusion of poly-L-lysine for as little as 10 seconds is enough to improve cell adherence to uncoated cover slips. We have added a line of explanation in the text (lines 137-138).

2. Regarding 4.3. Placing a cover slip onto another glass layer (bottom of the 35 mm dish) is a challenging setting if the user does not have access to a high NA objective. Maybe the authors might think of mentioning an alternative for that, like using a chamber system allowing for placing the cover slip without having an additional bottom.

We have added a note acknowledging this potential problem and providing a potential alternative (lines 143-148).

3. Regarding 5.1. The authors should define "empty". I suppose it is a clear glass surface without any membrane attached, but it would be nice to have a defintion for that.

We have modified this sentence to give a clearer definition (lines 184-186).

4. Regarding 5.4. The authors mention the "ANAP intensity of the first exposure in nucleotide-free solution". What is meant with first exposure? Is it the first data point in a time series? I recommend to be more explicit here.

We have made some changes to clarify this point. We have added an extra step in section 4 (lines 165-167) explicitly describing taking an initial exposure for the purposes of normalisation. We have then referred to this step in 5.4 (lines 197-199).

5. Regarding bleaching correction: The exact procedure of bleaching correction was not clear for me. The authors should be more specific about how the fitted time course is used to extrapolate the peak values.

We have modified section 5 (lines 200-210) and figures 3D-E (including the figure legend, lines 382-388) to try and clarify this process. We added an additional inset to figure 3D and

modified the inset in figure 3E to explicitly show peak fluorescence before and after bleaching correction.

6. The authors are comparing two variants of their approach.
6.1. It would be interesting to see the different binding data from unroofed cells compared to binding data from PCF. Don't mind that comment if this would be beyond the scope of this technical paper.

We have added an additional Figure 6 to show overlaid unroofing and PCF data from our previous publication (legend in lines 412-420). We discuss their similarity and differences in the text, as well as the generalizability of this finding to other experimental systems (lines 478-481).

6. It would be interesting to hear more about the preferences of one variant over the other. For instance regarding the required protein expression: Can you give a minimum number of channel proteins in the patch and in the unroofed membrane needed for a sufficient signal to be analyzed?

We discuss the merits of unroofed vs. PCF in various sections of the paper, including lines 315-325 and 474-481. We discuss the relationship between channel expression and signal strength in lines 489-497.

7. The authors might discuss their protocol in the light of using another fluorophore-tagged ATP derivative, published in 2013: Bhargava Y, Nicke A, Rettinger J. Validation of Alexa-647-ATP as a powerful tool to study P2X receptor ligand binding and desensitization. Biochem Biophys Res Commun. 23;438(2):295-300. doi: 10.1016/j.bbrc.2013.07.058.

We have added a reference to this paper and discussion of the use of Alexa-647 ATP in lines 505-509. Thank you for bringing this to our attention.

Reviewer #2:
Manuscript Summary:
The manuscript present a novel and uniquely powerful approach to simultaneously monitor the binding of fluorescent adenine nucleotides to intact functional transmembrane proteins. The authors elegantly incorporate fluorescent unnatural aminoacid ANAP and measure FRET between fluorescent trinitrophenyl nucleotide derivatives. Simultaneous fluorescence and current measurements allow simultaneous monitoring of ligand binding and change in protein function at unprecedented resolution. The manuscript as a whole is well written and easy to understand and follow. The data is of the highest quality. The method is of broad interest to the ion channel and GPCR community and this protocol is likely to help with broad

adaptation of this method by multiple laboratories.

Major Concerns:
None

Minor Concerns:
1. One of the most powerful aspects of this study is the ability to simultaneously record fluorescence and currents from a ripped-off patches. However, to quantify ANAP fluorescence, the authors obtain a spectral image. Does the presence of the borosilicate glass around the the patch pipet introduce spatial aberrations or blurring that might interfere with spectral decomposition? Presumably this is also important for robust FRET measurements.

We have observed spatial aberrations in our images, but this does not affect the shape of our spectra. We now discuss the challenges introduced by imaging fluorescence through the pipette glass in lines 238-241 in addition to our discussion of subtraction artefacts in Figure 5C-E (lines 242-245, 402-410, and 465-473) .

2. It would be helpful if the authors provided further details or parameters for optimal exposure time for patch clamp fluorometry experiments. Potentially one of the applications may be measurement of kinetic changes in fluorescence. However, this may be limited by long exposure times, it would be helpful to know potential temporal resolution.

We have added a note (lines 168-173) to discuss this point.

3. The presence of bulk fluorescent dye could introduce concentration-dependent FRET due to the presence of the fluorescent ligand near the receptor by random chance. Have the authors considered the potential contribution of concentration-dependent FRET in their experimental setup?

We discuss the confounding influence of non-specific ligand binding and appropriate controls in lines 444-464.

4. Figure 5 B right subpanel and C, it may be helpful to provide an axis with fluorescence wavelength instead of the scale bar for comparison with FIgure 4B.

We have added a wavelength axis to figures 5B,C.

Dear Michael,

Thank you for your email. Unless stated otherwise (e.g. explicitly in the figure legend), all eLife figures are published under the Creative Commons Attribution License (CC-BY-4.0)(https://creativecommons.org/licenses/by/4.0/), what this means you don't need to request permission and you're free to reproduce the material as long as you give appropriate credit.

So yes, it would be fine to reuse material from the published eLife article, provided that the original creator and source are credited. You'll also need to cite the license and provide the link to the license (this link https://creativecommons.org/licenses/by/4.0/). For full details about the CC-BY 4.0 license and how to cite/attribute the original source see https://creativecommons.org/licenses/by/4.0/

Best wishes,
Wei Mun

Wei Mun Chan
Editorial Manager, *eLife*